Journal of
Manufacturing and Materials Processing

MDPI

Article

Performance Analysis of FFF-Printed Carbon Fiber Composites Subjected to Different Annealing Methods

Javaid Butt [1,*], Md Ashikul Alam Khan [1], Muhammad Adnan [1] and Vahaj Mohaghegh [2]

[1] College of Engineering, Birmingham City University, Birmingham B4 7XG, UK; ashikul.khan@bcu.ac.uk (M.A.A.K.); muhammad.adnan@bcu.ac.uk (M.A.)
[2] Engineering Department, MGE (Colchester) Ltd., Colchester CO4 9HY, UK; vahaj.mohaghegh@mgelectric.co.uk
* Correspondence: javaid.butt@bcu.ac.uk

Abstract: Annealing is a popular post-process used to enhance the performance of parts made by fused filament fabrication. In this work, four different carbon-fiber-based composites were subjected to two different annealing methods to compare their effectiveness in terms of dimensional stability, surface roughness, tensile strength, hardness, and flexural strength. The four materials include PLA-CF, PAHT-CF, PETG-CF, and ABS-CF. The annealing methods involved heating the printed composites inside an oven in two different ways: placed on a tray and fluidized bed annealing with sharp sand. Annealing was conducted for a one-hour time interval at different annealing temperatures selected as per the glass transition temperatures of the four materials. The results showed that oven annealing provides better results under all scenarios except dimensional stability. PETG-CF and ABS-CF composites were significantly affected by oven annealing with expansion along the *z*-axis as high 8.42% and 18% being observed for PETG-CF and ABS-CF, respectively. Oven annealing showed better surface finish due to controlled and uniform heating, whereas the abrasive nature of sand and contact with sand grains caused inconsistencies on the surface of the composites. Sand annealing showed comparable hardness values to oven annealing. For tensile and flexural testing, sand annealing showed consistent values for all cases but lower than those obtained by oven annealing. However, oven annealing values started to decrease at elevated temperatures for PETG-CF and ABS-CF. This work offers a valuable comparison by highlighting the limitations of conventional oven annealing in achieving dimensional stability. It provides insights that can be leveraged to fine-tune designs for optimal results when working with different FFF-printed carbon-fiber-based composites, ensuring better accuracy and performance across various applications.

Keywords: additive manufacturing; fused filament fabrication; annealing; PLA; PETG; ABS; PAHT; carbon fiber

Citation: Butt, J.; Khan, M.A.A.; Adnan, M.; Mohaghegh, V. Performance Analysis of FFF-Printed Carbon Fiber Composites Subjected to Different Annealing Methods. *J. Manuf. Mater. Process.* **2024**, *8*, 252. https://doi.org/10.3390/jmmp8060252

Academic Editor: Guido Di Bella

Received: 6 October 2024
Revised: 28 October 2024
Accepted: 6 November 2024
Published: 11 November 2024

1. Introduction

The maturation of additive manufacturing (AM) methods has made them an integral part of different industrial sectors, including automotive, aerospace, bioprinting, textiles, electronics, and medical [1–3]. AM methods are characterized by faster prototyping, reducing product development cycles, and enabling rapid iteration and customization [4]. They are creating a massive impact in the world around us and in space as well. A remarkable example is the European Space Agency's use of metal AM technology to produce the first metal part ever manufactured in space [5]. Another one is focused on a self-winding mechanical watch specifically designed to meet NASA's standards for activities conducted by astronauts both inside and outside a spacecraft [6]. These AM examples in space exploration are offering solutions for manufacturing in extreme environments where conventional methods are impractical. There are seven categories of AM as per ISO/ASTM 52900:2021. They include binder jetting, directed energy deposition, material extrusion,

material jetting, powder bed fusion, sheet lamination, and vat polymerization [7]. Out of these seven categories, material extrusion is one of the most used methods due to its ease of operation, cost-effectiveness, and range of material availability [8]. Fused filament fabrication (FFF), also known as fused deposition modeling (FDM), is a material extrusion process that uses thermoplastics to print parts by depositing melted material through a heated nozzle layer by layer. However, there are some common challenges associated with FFF due to the layer-by-layer deposition nature, including rough surface finish with visible lines, dimensional inaccuracies, and limited mechanical performance, thus limiting their applicability [9]. There are different ways of overcoming these challenges such as optimization of process parameters, addition of fibers/particles, and post-processing operations. Process parameters with significant impact on FFF-printed parts include extrusion temperature, print speed, line width, layer height, infill pattern/percentage, and print orientation [10,11]. In this context, Butt et al. [12] investigated the effects of layer heights and line widths on four different FFF-printed thermoplastics (Premium PLA, Graphene Enhanced PLA, ABS Extrafill, and ASA Extrafill). They showed the limitations associated with the default printing settings (0.2 mm layer height and 0.4 mm line width) and how layer height as well as line width can be optimized to achieve desired properties in FFF-printed parts. Shakeri et al. [13] examined the influence of thickness, infill pattern, number of walls, and layer height on cylindricity and circularity of FFF-printed Nylon (PA6) parts. They concluded that a hexagonal infill pattern, thickness of 5 mm, wall layer of 2, and layer height of 1.125 mm were the optimal process parameters for circularity and cylindricity in experiments. They also developed a linear regression model to observe the relationship between the control variables with cylindricity and circularity, with the confirmation test showing a 95% acceptance. Vidakis et al. [14] analyzed the impact of six printing parameters on overall energy printing consumption (EPC), the specific printing energy (SPE), and specific printing power (SPP) for FFF-printed ABS. They discussed the multi-factor effects and presented quadratic regression models with ANOVA for the six printing parameters that show effectiveness for EPC and SPE but not for SPP. Such studies also emphasize the significance of optimizing process parameters to promote smart, sustainable, and green manufacturing.

The second option to enhance the performance of FFF-printed parts is the incorporation of particles, fibers, or nanomaterial reinforcements to form composite materials [15,16]. Abderrafai et al. [17] investigated the effects of carbon fibers concentration and type, infill pattern, and environmental temperatures on FFF-printed Polyamide 12. They observed an increase of 6.3 times in tensile modulus and 2.15 times for tensile strength, compared to unreinforced material. They also reported that addition of carbon fibers into a PA12 matrix improves both its stiffness and strength but reduces the ductility. Similarly, Chicos et al. [18] studied the influence of infill density on mechanical and thermal properties of short carbon-fiber-reinforced polyamide composites. They reported the highest tensile and flexural strengths as well as lowering of glass transition temperature at 100% infill and 25% infill, respectively. They also recorded lower temperatures of onset degradation at high infill densities (100% and 75%) compared to lower ones (50% and 25%). Therefore, addition of carbon fibers can enhance mechanical properties, making the products more applicable for load-bearing engineering applications. However, optimization of processing parameters cannot be overlooked.

Identification and utilization of effective post-processing operations is the third option that can enhance the performance of FFF-printed parts. Annealing is a popular post-process that can relieve internal stresses and enhance the properties of thermoplastics. Arjun et al. [19] investigated the effect of process parameters and thermal annealing on the tensile strength of FFF-printed composite carbon fiber PLA. They reported an increase of 14% in tensile strength based on a set of optimal combinations that include an infill density of 90%, gyroid printing pattern, 230 °C nozzle temperature, 0.1 mm layer height, 40 mm/s print speed, and annealing at 95 °C for 120 min. This work highlights the effectiveness of optimizing the process parameters and utilizing post-processing methods to enhance mechanical properties. Bhandari et al. [20] analyzed the impact of different annealing

temperatures and time intervals on the tensile properties of PETG-CF and PLA-CF. They showed that the interlayer tensile strength of PETG-CF and PLA-CF composites increased by three times and two times, respectively. Annealing for longer durations shows better results but temperatures vary as PLA-CF showed a major increase in interlayer tensile strength at 90 °C, whereas the same was observed for PETG-CF at 120 °C. Seok et al. [21] studied the effects of annealing for strength enhancement of FDM-printed ABS reinforced with recycled carbon fiber (rCF) content of 10 wt% and 20 wt%. They used three different annealing temperatures (105 °C, 125 °C, and 175 °C) and time intervals (0.5 h, 2 h, and 4 h). They reported an increase in tensile and flexural strengths with 20 wt% rCF at 105 °C and 175 °C, respectively. This work not only highlights the impact of annealing but also sheds light on the effect of recycling carbon fibers, promoting sustainability and cost-effectiveness efforts.

Given the significant importance of mechanical performance in critical applications, understanding the influence of annealing on FFF-printed composites is crucial. Moreover, it is critical to analyze the effectiveness of different annealing methods on the performance of composite materials. This can provide an alternative to the conventional oven annealing to ensure desired properties in FFF-printed parts. Therefore, this paper aims to analyze and compare the effects of two annealing methods on the performance of four composite thermoplastics. By identifying the optimal annealing parameters for two different methods, this study seeks to provide valuable insights into improving the performance and reliability of FFF-printed carbon fiber composites for different engineering applications.

2. Methodology

2.1. Material and Manufacturing Process

Four different thermoplastics reinforced with carbon fibers were used in this work. They include PLA, nylon, PETG, and ABS. From here onwards, they will be referred to as PLA-CF [22], PAHT-CF [23], PETG-CF [24], and ABS-CF [25]. The first three composites were sourced from Bambu Lab (Shenzen, China) and the fourth was purchased from IEMAI 3D (Guangdong, China). The composites were printed using Bambu Lab X1E 3D Printer (Shenzen, China) with a build volume of 256 × 256 × 256 mm^3, air purification, and active chamber heating. Three different parts were manufactured, and their dimensions were based on British and International Standards. They include a BS EN ISO 527-2:2012 tensile test sample [26], a BS EN ISO 868:2003 hardness test sample [27] and a BS EN ISO 178:2019 three-point flexural testing sample [28]. All the composites were printed in the flat orientation with the same settings of speed as 50 mm/s, 100% infill with rectilinear pattern, 100% flow, 0.2 mm layer height, and 0.4 mm nozzle. The printing parameters relevant to the material are shown in Table 1.

Table 1. Printing parameters for composites.

#	Materials	Nozzle Temperature (°C)	Bed Temperature (°C)
1	PLA-CF	230	45
2	PAHT-CF	290	100
3	PETG-CF	255	70
4	ABS-CF	240	95

2.2. Annealing Methods

The composite materials were subjected to two different annealing methods inside a Thermo Scientific Heraeus Oven (Nottinghamshire, UK). The annealing time interval was one hour [29], with temperatures as shown in Table 2. The annealing temperatures were chosen as per the glass transition temperature (Tg) of the four materials to ensure a structured approach for assessing the response of the materials across a range of thermal exposures. As shown in Table 2, four different temperatures were chosen. The first temperature is below the Tg to serve as a control point to observe any pre-Tg physical changes without inducing substantial molecular motion, allowing the polymer chains to remain

relatively fixed. At this temperature, stress relief could still occur gradually, providing insight into any minor changes in the internal stress distribution without significant softening. The second temperature value is at the Tg where the softening process would initiate, enabling chain mobility and relaxation of internal stresses. This can lead to increased ductility and potentially affect surface and bulk properties while allowing the material to retain structural stability. The third temperature value is above Tg where chain mobility increases, allowing for further relaxation and realignment of polymer chains. The fourth temperature is well above the Tg and is expected to maximize molecular rearrangement without degrading the material. At this higher temperature, the polymer chains can realign and potentially even improve mechanical properties. This gradient approach to annealing helps characterize the mechanical and thermal responses of the materials at strategic points relative to Tg, offering a clear profile of how each temperature affects stress relief, stability, and overall material performance.

Table 2. Annealing temperatures for the composites (* glass transition temperature, °C).

Materials	Annealing Temperatures (°C)
PLA-CF	53 63 * 73 83
PAHT-CF and PETG-CF	60 70 * 80 90
ABS-CF	95 105 * 115 125

For annealing, the samples were placed in the oven according to the specified annealing methods and subjected to the designated temperature and duration. After the annealing time elapsed, the oven was turned off and the samples were left to cool inside the oven until they reached room temperature. The first method was conventional annealing, where the samples were placed on a tray (L × W × H; 300 mm × 210 mm × 40 mm) and placed in the oven at a specified temperature, then allowed to cool after the time has elapsed. The second method was fluidized bed annealing with sharp sand (will be referred to as sand annealing), and the samples were submerged in the sand bed to be uniformly annealed. The tray was filled with sand to a height of 30 mm and the samples were placed midway deep in the sand. For this work, sharp sand was used, which typically contains larger particles with angular edges. The angular shape of the particles in sharp sand allows for better contact between them, which promotes more efficient heat transfer. The two annealing methods present a different way of heating the samples and each method offers unique advantages in terms of heat transfer and temperature control, with the controlled cooling process playing a crucial role in minimizing residual stress and enhancing mechanical properties.

2.3. Measurements and Experimental Testing

All the measurements were taken before and after annealing to ascertain the impact of annealing on the samples. K-type thermocouples, with an operating range of −100 °C to 500 °C, were fixed to the surface of the samples with heat resistant Kapton tape. They were connected to a data logger OM-HL-EH-TC 3927 (Omega, Norwalk, CT, USA) and the temperature distribution on the samples was recorded starting from room temperature to annealing and finally coming back to room temperature after cooling.

The dimensions of the dog-bone tensile samples were measured using a digital Vernier caliper and surface roughness analysis was undertaken using a Mitutoyo Surftest SJ-210

(Andover, UK) contact-type surface profilometer [30] as per ISO 21920-2:2021 [31]. Three measurements were taken on each sample with a measuring speed of 0.5 mm/s. After surface analysis, the dog-bone samples were subjected to tensile test on an INSTRON 3382 Universal Testing Machine with a speed of 1 mm/min as per BS EN ISO 527-2:2012 [26].

The square samples were subjected to indentation hardness as per BS EN ISO 868:2003 [27] using a Shore D durometer. The indentation was measured on five different points to obtain an average hardness value. The hardness test was followed by three-point flexural testing of the rectangular sample on an INSTRON 3382 Universal Testing Machine with a speed of 2 mm/min as per BS EN ISO 178:2019 [28].

3. Results and Discussions

3.1. Dimensional Analysis

Shrinkage or expansion of thermoplastics is common post annealing due to the relaxing of the internal stresses [29,32]. The changes could be observed along any of the three axes (x, y, and z) and were attributed to the way FFF-printed samples cool, where internal tensions, stresses, and entrapped air bubbles become locked between the layers during the solidification process. The dimensions of the four composites were measured using a digital Vernier caliper and their deviations for the two annealing methods are shown in Table 3.

Table 3. Dimensional analysis for the composites.

Materials	Annealing Temperature (°C)	Oven Annealing			Sand Annealing		
		Length (%)	Width (%)	Thickness (%)	Length (%)	Width (%)	Thickness (%)
PLA-CF	53	−0.12	0.63	−0.75	−0.29	−0.25	2.50
	63	−0.29	1.75	−1.25	−1.76	−0.25	2.83
	73	−0.59	1.37	0.25	−2.35	−0.85	4.92
	83	−2.35	−1.23	2.75	−2.94	−0.60	6.92
PAHT-CF	60	−0.59	2.73	2.67	−0.59	2.20	1.83
	70	−0.59	2.33	2.75	−0.59	2.58	2.33
	80	−0.59	1.65	3.83	−0.59	2.73	2.75
	90	−1.18	2.78	5.75	−1.18	2.58	2.92
PETG-CF	60	−0.59	0.55	1.33	−0.59	0.50	0.67
	70	−1.18	0.23	2.33	−1.18	0.18	1.50
	80	−2.35	−0.90	3.58	−1.76	−0.40	2.08
	90	−3.65	−2.30	8.42	−2.35	−0.63	3.33
ABS-CF	95	−1.18	0.27	2.17	−1.18	0.78	0.25
	105	−2.94	−1.02	6.58	−1.18	0.52	1.42
	115	−5.29	−3.15	14.75	−2.35	−1.68	7.42
	125	−7.65	−4.77	18.08	−3.53	−1.90	7.58

It is clear from Table 3 that the highest variations were observed at the highest annealing temperatures. This is due to the material softening more at elevated temperatures, causing greater changes in size as internal stresses are released unevenly. Along the y-axis (width), PLA-CF experienced almost twice the shrinkage with oven annealing (1.23%) compared to sand annealing (0.6%). The values were comparable for changes along the x-axis (length). However, the major difference was observed along the z-axis (thickness) as sand annealing showed an expansion of 6.92% compared to 2.75% for oven annealing. It is to be noted that the difference in heat distribution between sand annealing and oven annealing plays a significant role in the crystallization behavior and thermal expansion

of PLA-CF. Oven annealing generally provides more uniform heating due to controlled convection, allowing for consistent crystallization and slower thermal expansion across the material. This uniform heat exposure encourages gradual crystallization, which reinforces the polymer matrix and contributes to improved mechanical properties [29,32]. The temperature distribution data between oven and sand annealing is shown in Figure 1. For sand annealing, a more gradual temperature rise and cooling cycle can be observed in Figure 1 due to the thermal insulating effect of the sand particles. This gradual heating minimizes thermal shock, facilitates stable crystallization, and reduces overall internal stresses as well as dimensional distortions. However, the pronounced directional sensitivities of PLA-CF composites can lead to anisotropic expansion during sand annealing due to uneven heat absorption. This effect is especially noticeable along the *z*-axis, where the material flow is more constrained during FFF, thereby intensifying dimensional changes in that direction. Additionally, due to PLA's lower glass transition temperature (63 °C) and higher susceptibility to thermal degradation, sand annealing can cause localized expansion along the *z*-axis. These expansions may not fully revert during cooling, resulting in dimensional changes after thermal treatment [33]. This effect is more pronounced in PLA-CF than in higher-temperature-resistant materials like PETG-CF or PAHT-CF, which exhibit better stability due to their inherently higher crystallinity potential and thermal resistance.

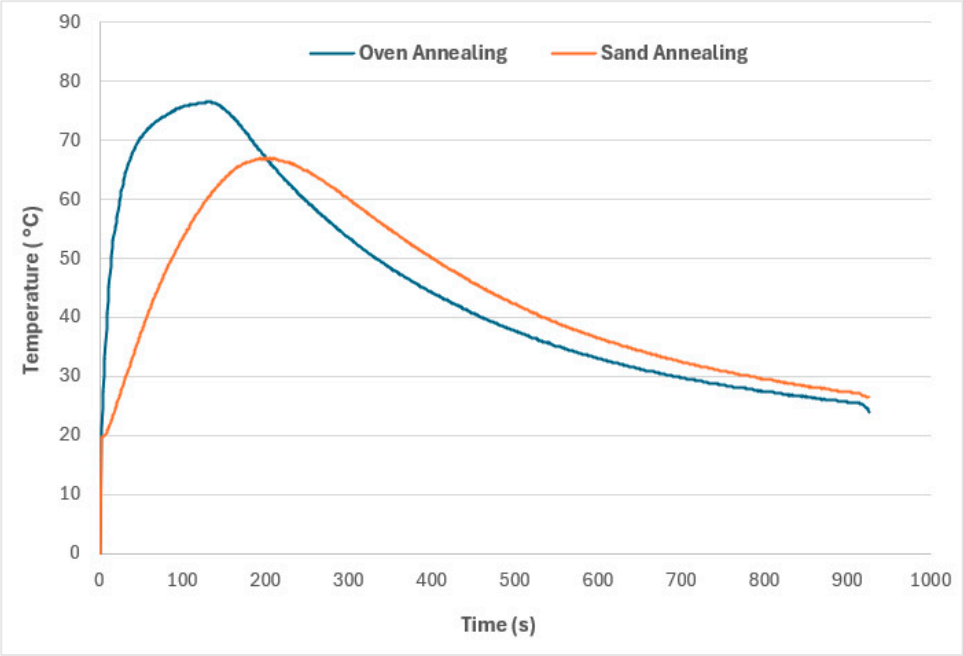

Figure 1. Temperature distribution for PLA-CF during annealing at 83 °C for 1 h, followed by cooling.

For PAHT-CF, both annealing methods showed similar values for length and width. However, the main difference was observed for the thickness (*z*-axis) where the expansion increased with high annealing temperature. At 90 °C, sand annealing showed an expansion of 2.92% compared to 5.75% for oven annealing. This demonstrates the dimensional stability provided by sand annealing due to the extra support of the sand particles during the annealing process. This contrasts with PLA-CF, where sand annealing showed more expansion, thus highlighting the effectiveness of different annealing methods. The same pattern was observed for both PETG-CF and ABS-CF, with sand annealing showing exceptional dimensional stability at all temperatures along the three axes. The highest expansion for PETG-CF for oven annealing was 8.42%, compared to 3.33% for sand annealing. For ABS-CF, 18.08% expansion was observed for oven annealing, compared to 7.58% for sand annealing. These results make sand annealing better suited for the composite materials when dimensional stability is a prime consideration, except for PLA-CF due to its inherent

material properties. Sand annealing provides a more uniform heating across the surface of the samples, while oven annealing provides a more gradual, less direct heat exposure. In the case of PLA-CF, this localized heating in the sand bed could promote more thermal expansion, resulting in a greater thickness increase, especially since the material is sensitive to both crystallization and expansion during heat treatment [33,34]. Overall, sand annealing showed better dimensional stability for all materials (except PLA-CF) by physically constraining the parts and preventing excessive deformation during softening.

3.2. Surface Roughness Analaysis

The FFF-printed composite samples were submerged in sand and placed in a tray to be annealed inside an oven. Contact with sand could have adverse effects on the surface roughness of the samples due to abrasion. Moreover, the layer-by-layer nature of the FDM process introduces distinct layer lines, which exacerbate the challenges associated with achieving a smooth surface finish [12,35,36]. Therefore, this test was performed to assess the impact of varying annealing conditions and contact media on the surface roughness of the composite samples. For this purpose, a Surftest SJ-210 (Mitutoyo, Kawasaki, Japan) contact-type surface profilometer was used and all the samples were measured with the traverse direction being diagonally across the building direction at an angle of 45°. The average surface roughness (Ra) values measured along the length of the samples are shown in Figure 2.

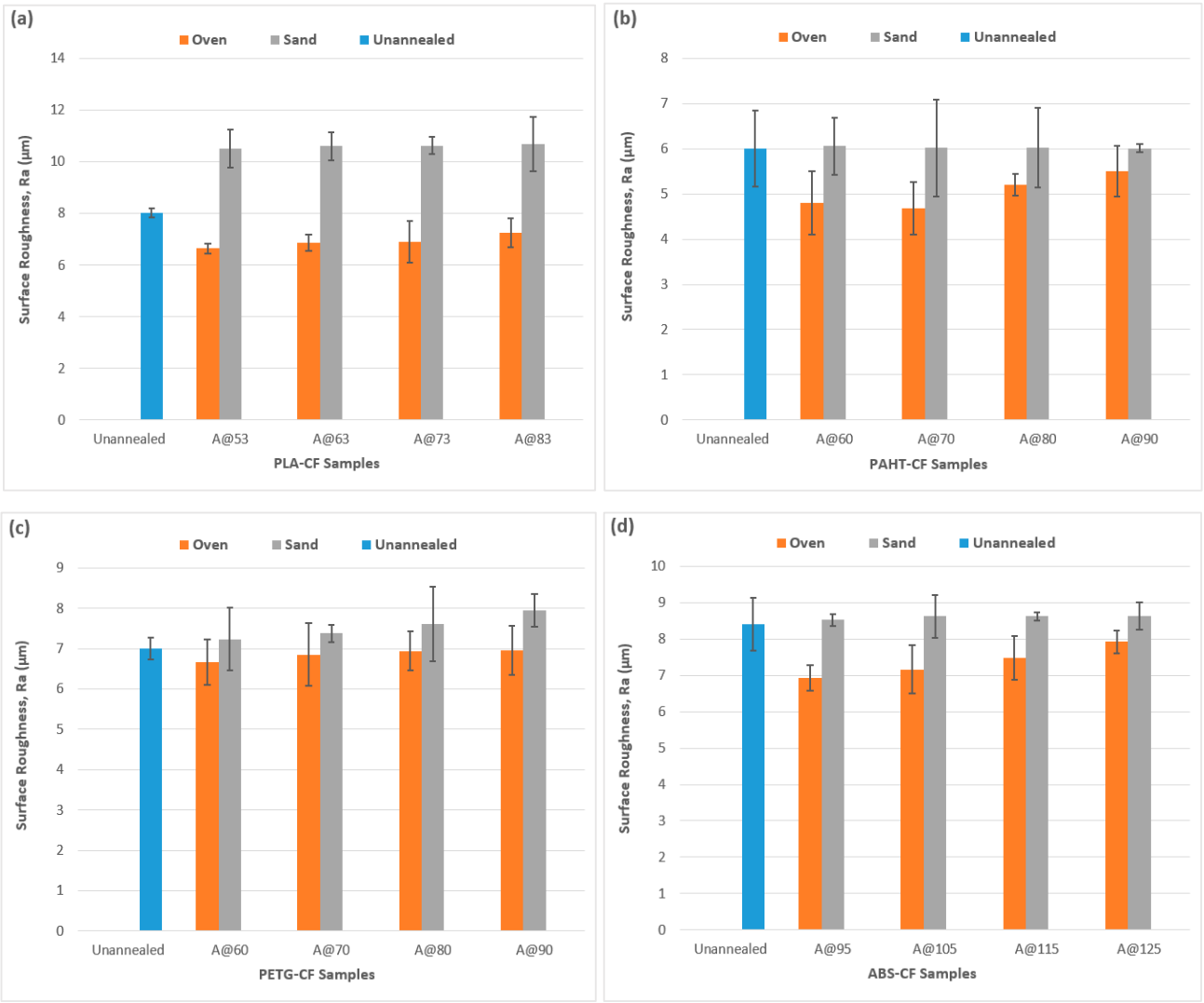

Figure 2. Surface roughness measurements: (**a**) PLA-CF; (**b**) PAHT-CF; (**c**) PETG-CF; (**d**) ABS-CF.

The surface roughness results from Figure 1 show that oven annealing yielded lower surface roughness values compared to unannealed as well as sand annealed samples. This is because oven annealing tends to provide better control over the annealing process, leading to more uniform surface finishes due to consistent heating. On the other hand, sand annealing, while better for dimensional accuracy (Section 3.1), led to higher surface roughness due to physical contact with sand grains and abrasions. In the case of PLA-CF (Figure 2a) and PAHT-CF (Figure 2b), oven annealing showed significantly lower surface roughness values compared to sand annealing. However, these improvements were observed at lower temperatures with surface smoothing due to recrystallization and softening while worsening at high temperatures due to expansion and uneven shrinkage [35]. Sand annealing for PLA-CF and PAHT-CF showed higher but consistent values at all temperatures, indicting a controlled albeit ineffective process to improve surface finish.

For PETG-CF (Figure 2c), the oven annealing values were consistent but only slightly lower than unannealed samples. The lowest value of 6.6 µm (compared to 7 µm for unannealed samples) was observed at 60 °C, meaning that the surface roughness of PETG-CF samples was not significantly affected by annealing. Surface roughness values for sand annealing were higher than oven annealing and kept increasing with high temperatures, with a value of 7.9 µm at 60 °C. ABS-CF (Figure 2d) showed better surface finish due to better layer adhesion at lower oven annealing temperatures. However, higher temperatures led to an increase in roughness values due to uneven shrinkage and fiber movement. The lowest value of 6.9 µm and the highest value of 7.9 µm (compared to 8.4 µm for unannealed samples) were observed at oven annealing temperatures of 95 °C and 125 °C, respectively. Sand annealing surface roughness values were consistent and comparable to annealed samples. It is clear from these results that oven annealing at lower temperatures is better suited for good surface finish because it offers more controlled and uniform heating, leading to fewer thermal gradients, reducing warping and uneven surface textures [19–21]. On the other hand, the abrasive nature of sand and contact with sand grains cause inconsistencies on the surface of the samples during sand annealing, leading to poor surface finish.

3.3. Tensile Testing

Annealing is an established post-process used to improve the tensile properties of thermoplastics [19,20,29] and this work is comparing two different methods to ascertain the impact on the tensile strength of four carbon fiber composites. The results of the tensile testing are shown in Figure 3. Both methods demonstrated higher values compared to unannealed samples, highlighting the positive effects of annealing. Figure 3a shows a gradual increase in tensile strength with increased annealing temperatures for both methods. However, the increase is more significant in the case of oven annealing compared to sand annealing. The highest values were observed at the highest temperature of 83 °C, indicating that the heat helped in relieving internal stresses and promoting better layer bonding [19,34]. An increase of 23.2% was observed for oven annealing at 83 °C, compared to unannealed PLA-CF. On the other hand, an increase of 13% was observed for sand annealing at the same temperature, highlighting the effectiveness of oven annealing. A similar pattern was observed for PAHT-CF (Figure 3b), with the tensile strength increasing with increased annealing temperature. Polyamide benefits from annealing-induced crystallization due to improvement in crystallinity and stabilization of the internal structure [37]. The highest increase was observed at 90 °C as 26% for oven annealing, compared to unannealed PAHT-CF. The increase in tensile strength for sand annealing was only 8.6% at the same annealing temperature. These results show the effectiveness of oven annealing to increase tensile strength for the two semi-crystalline materials.

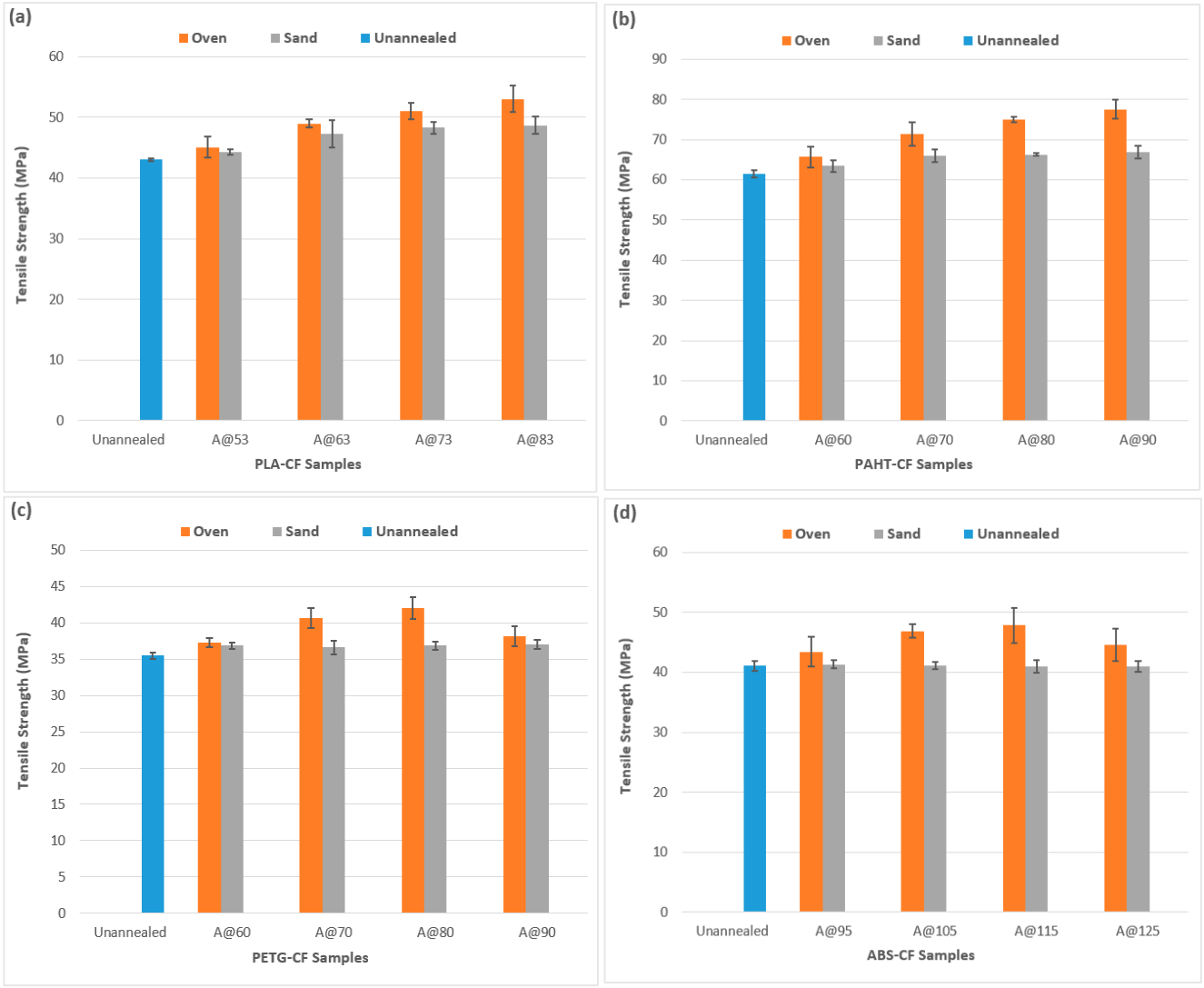

Figure 3. Tensile testing results: (**a**) PLA-CF; (**b**) PAHT-CF; (**c**) PETG-CF; (**d**) ABS-CF.

A different pattern was observed for the two amorphous materials. PETG-CF showed an increase in tensile strength to a certain annealing temperature before sharply declining. Tensile strength increased until 80 °C, showing an increase of 18.3% for PETG-CF (Figure 3c). However, there was a sharp decline at 90 °C, indicating that excessive temperature can soften the material without significantly increasing strength [38]. There was minimal increase in tensile strength for sand annealing, with the values staying consistent through all the annealing temperatures. ABS-CF experienced the highest dimensional deformation along the *z*-axis (Section 3.1) for oven annealing. Despite these changes in dimensions, no significant improvements in tensile strength were observed. The highest tensile strength was observed at 115 °C, showing an increase of 16.5% (Figure 3d), compared to unannealed ABS-CF. The tensile strength decreased at 125 °C, indicating limited improvement in interlayer adhesion at elevated temperatures [39]. On the other hand, sand annealing did not demonstrate any significant changes in tensile strength.

The distinct heat transfer and thermal conductivity properties between sand and oven annealing impact the tensile strength of semi-crystalline (PLA-CF, PAHT-CF) and amorphous (PETG-CF, ABS-CF) composites due to differences in temperature uniformity and rate of thermal exposure. Oven annealing provides more uniform heat distribution, which is beneficial for semi-crystalline composites like PLA-CF and PAHT-CF. This even heating enhances molecular alignment and crystalline structure, improving tensile strength

by reducing residual stresses and enabling more complete crystallization [29,32]. In contrast, sand annealing typically leads to more gradual heating and cooling, but it can create localized hot spots due to sand's lower thermal conductivity. For semi-crystalline materials, this may disrupt uniform crystallinity formation and lead to weaker interlayer bonding, resulting in lower tensile strength increase compared to oven-annealed samples. For amorphous materials, however, the gradual temperature change in sand annealing generally has less impact on their non-crystalline structure, leading to more consistent mechanical properties regardless of the method. These results indicate that oven annealing is more suited to enhance the tensile strength of both semi-crystalline and amorphous materials, with the former showing a more significant increase compared to the latter due to their sensitivity to thermal treatment and inherent crystalline structure.

3.4. Hardness Testing

Oven annealing has been shown to impact the surface hardness of thermoplastics [29,38]. However, sand annealing with the irregular contact and abrasive nature of the sand could lead to different results. Therefore, it is crucial to assess the hardness of the four composites to ascertain the effects of the two annealing methods. It is to be noted that annealing temperatures and time intervals can affect the hardness values. An average of five values were taken from each square sample, equidistant from each other. The results of Shore D hardness are shown in Figure 4. It is evident that annealed samples for both methods showed higher values compared to the unannealed ones, indicating the positive effect of annealing.

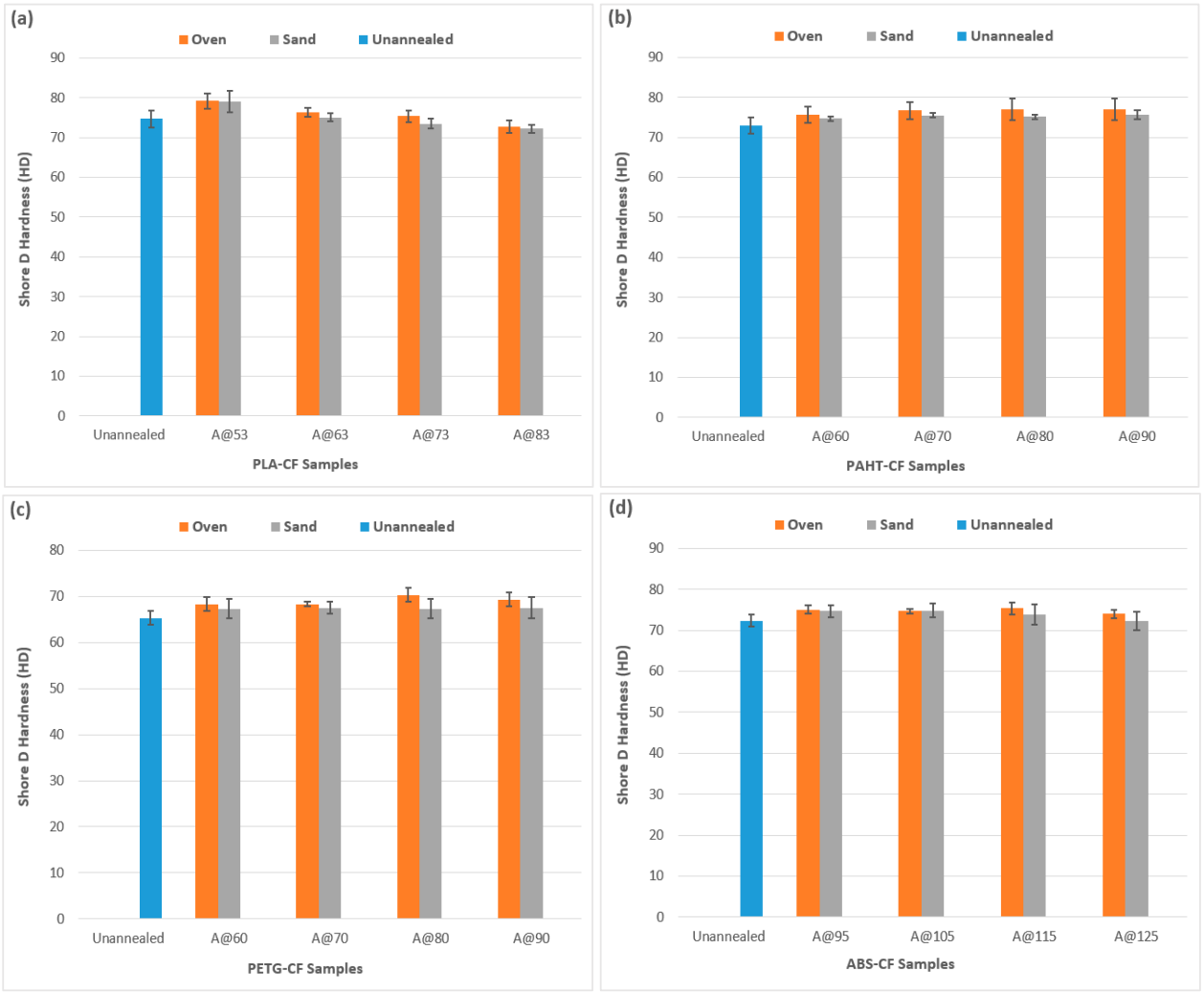

Figure 4. Hardness testing results: (**a**) PLA-CF; (**b**) PAHT-CF; (**c**) PETG-CF; (**d**) ABS-CF.

As seen in Figure 4a, the hardness values peaked at the lowest annealing temperature of 53 °C for both oven and sand annealing. This is also consistent with the surface roughness and dimensional analysis where the smallest surface roughness (Section 3.2) and dimensional deviation (Section 3.1) were observed at the lowest annealing temperature. As the temperature increased, the hardness values decreased for both methods due to material softening. It is important to note that oven annealing yielded slightly higher values compared to sand annealing at all temperatures. The highest oven annealing values showed an increase of 6% compared to unannealed PLA-CF samples. In case of PAHT-CF (Figure 4b), the hardness values increase slightly as the temperatures increased, with the highest values being observed at the highest temperature of 90 °C for both oven and sand annealing. Compared to unannealed PAHT-CF samples, oven annealing resulted in a 5.4% increase, while sand annealing led to a 3.5% increase.

PETG-CF samples (Figure 4c) showed a similar pattern to their tensile testing with the highest values being observed at 80 °C before declining. Oven annealing showed the highest increase of 7.6% at 80 °C for oven annealing (compared to unannealed PETG-CF samples) whereas sand annealing demonstrated consistent values at all temperatures. However, the standard deviation of sand annealed samples was higher compared to over annealed ones due to the localized variations resulting from the sand's uneven thermal conductivity. ABS-CF (Figure 4d) demonstrated the same behavior as PETG-CF with the hardness values initially increasing before sharply declining. The highest values showed an increase of 4.1% (compared to unannealed ABS-CF samples) at 115 °C before decreasing to 2.3% at 125 °C. It is evident that hardness values did not increase significantly due to annealing, but oven annealing proved to be effective in enhancing the surface hardness to a larger extent compared to sand annealing. This is due to sand annealing's variable thermal conductivity and irregular surface contact that can result in localized cooling rates, which may lead to non-uniform hardness.

3.5. Flexural Testing

Three-point flexural testing has been used in this work to ascertain the flex or bending properties of the FFF-printed composites. The results from the testing are shown in Figure 5. All annealed samples showed higher values compared to their unannealed counterparts [38]. It is to be noted that oven annealing yielded higher flexural strength compared to sand annealing in all cases and the values increased with rising annealing temperature. For PLA-CF (Figure 5a), an increase of 17.3% was observed at the highest annealing temperature of 83 °C, compared to the unannealed samples. On the other hand, sand annealing only showed an increase of 9.2% at the same temperature. This is a common theme in flexural testing for all materials. Oven annealing demonstrated an increase in flexural strength with rising annealing temperatures, but the increase is less significant compared to oven annealing. This can be attributed to the uniform heat distribution that allows for better bonding between layers and stress relief during oven annealing. However, sand annealing can present varying thermal conductivity and inconsistencies due to uneven sand distribution, leading to less reliable improvements. Figure 5b showed that the flexural strength of PAHT-CF samples increased by 21.3% (at the highest annealing temperature) compared to unannealed PAHT-CF samples, whereas sand annealing only showed an increase of 8.2%. At the highest temperature of 90 °C, annealed PETG-CF samples (Figure 5c) showed an increase of 17% and 9.6% for oven annealing and sand annealing, respectively. Annealed ABS-CF samples (Figure 5d) showed the highest increase of 20% at 125 °C for oven annealing as opposed to 11.4% for sand annealing, compared to unannealed samples. These results indicate the effectiveness of oven annealing for enhancing the flexural strength of FFF-printed carbon fiber composites.

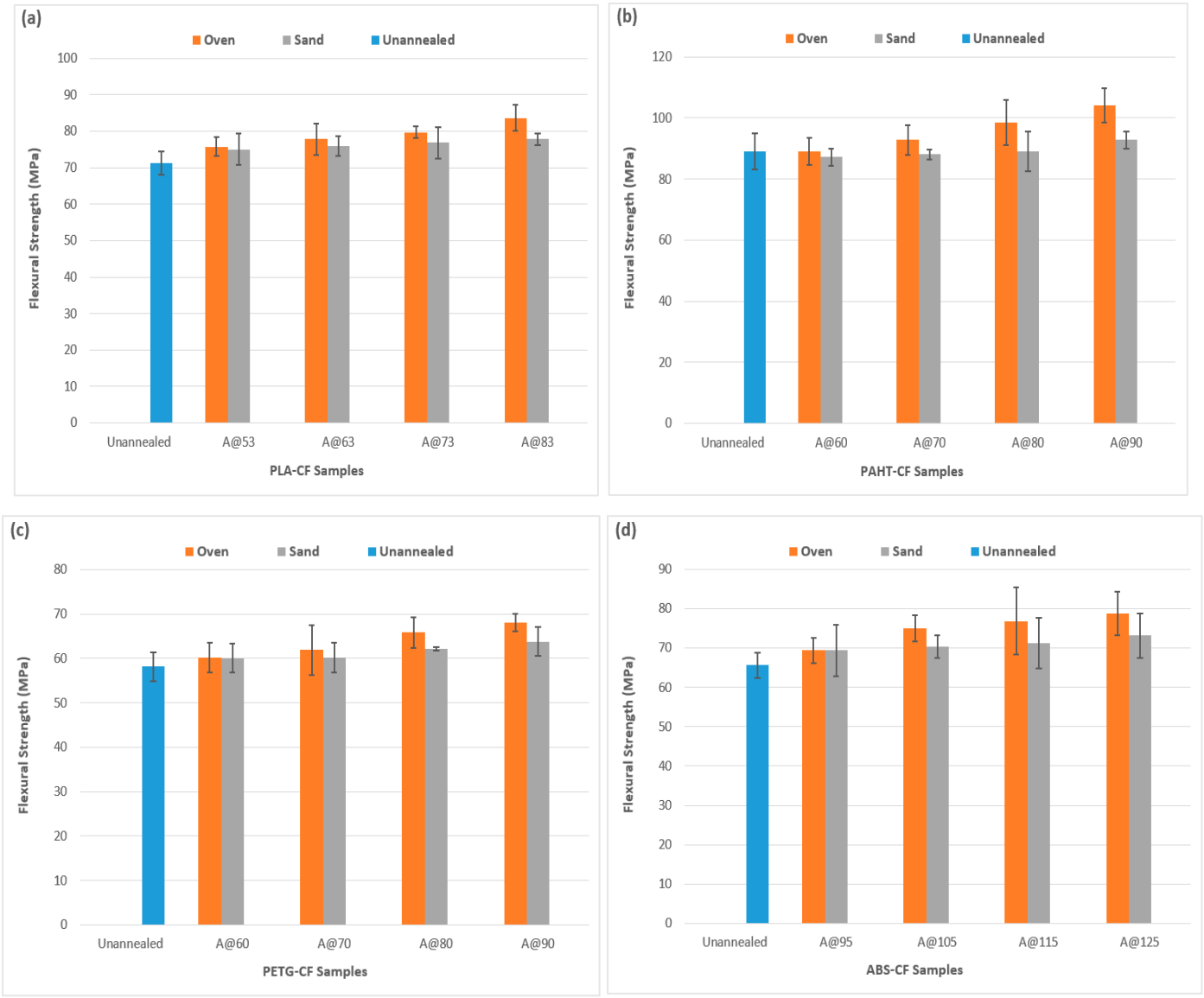

Figure 5. Three-point flexural testing results: (**a**) PLA-CF; (**b**) PAHT-CF; (**c**) PETG-CF; (**d**) ABS-CF.

4. Material Quality Characterization

It is important to highlight the limitations of the different methods to ensure optimal results can be achieved. This work is focused on four carbon-fiber-based composites manufactured by FFF and subjected to two different annealing methods. The preceding sections have demonstrated the effect of these methods on dimensional accuracy, surface roughness, tensile, hardness, and flexural performance with varying degrees of effectiveness. Therefore, it is imperative to identify the optimal set of parameters to achieve the desired properties in PLA-CF, PAHT-CF, PETG-CF, and ABS-CF parts. It has been observed that the semi-crystalline materials (PLA-CF and PAHT-CF) behave differently from the amorphous ones (PETG-CF and ABS-CF) due to their structure and response to heat. In the case of semi-crystalline materials, PAHT-CF is a high-temperature engineering-grade carbon-fiber-reinforced nylon, designed for high strength-to-weight ratio and excellent temperature resistant applications. Examples include aircraft components like brackets, housings, and ducts, as well as industrial tooling such as jigs, fixtures, and molds.

As per the results reported in this study, if the focus is on mechanical properties (tensile, hardness, flexural), then oven annealing should be the preferred choice. However, to produce a more robust final product, additional considerations should be made for

surface roughness and dimensional stability. Including these parameters will help in delivering a more complete solution that meets both functional and aesthetic requirements for high-performance applications. To better represent the parameters with the annealing temperatures, overlay contour plots for oven and sand annealing are shown in Figure 6. The black in-lines represent the overlay contour for flexural strength, whereas the red in-lines show the percentage difference for the *z*-axis (thickness). In this context, consider that a PAHT-CF product is required with a high dimensional stability (Table 3), maximum surface roughness of 6.1 µm, tensile strength of over 66 MPa, hardness of over 75 HD, and flexural strength of more than 89 MPa. While most oven annealing scenarios are well-suited for this application, they fall short in delivering the desired dimensional stability (as shown in Table 4), especially at elevated temperature of 90 °C where sand annealing showed an expansion of 2.92% compared to 5.75% for oven annealing along the *z*-axis (thickness). Therefore, sand annealing is the preferred choice for applications requiring high dimensional stability. As can be seen in Table 4, either of the two annealing temperatures can be chosen for the product as the difference between the two is minimal.

Table 4. Description of optimal combinations for PAHT-CF.

Annealing Method	Annealing Temperature (°C)	*z*-Axis (%)	Surface Roughness (µm)	Tensile Strength (MPa)	Hardness (HD)	Flexural Strength (MPa)
Oven	70	2.75	4.6	71.4	76.6	92.8
	80	3.83	5.2	75	77	98.4
	90	5.75	5.5	77.5	77	104
Sand	80	2.75	6.0	66.2	75.1	89
	90	2.92	6.0	66.8	75.6	92.8

Sand annealing is superior to oven annealing in terms of maintaining dimensional integrity (except PLA-CF). However, if the focus is shifted to exclude dimensional stability as it is a serious issue for all the oven annealed materials (except PLA-CF), then the outcome would be different. Figure 7 shows the overlayed contour plots for the amorphous material PETG-CF. This material delivers smooth and consistent print quality. The addition of carbon fiber enhances mechanical properties by providing a unique texture and significantly improved strength. These features make it especially well-suited for high-stress applications where both durability and a premium surface finish are critical. Typical examples include protective casings and automotive interior components such as mounts and brackets. For a PETG-CF product, consider a maximum surface roughness of 7.4 µm, tensile strength of over 36 MPa, hardness of over 75 HD, and flexural strength of more than 87 MPa. In this case, all the oven annealing scenarios fulfil the requirements, as opposed to only two sand annealing scenarios (at 70 °C and 80 °C), making oven annealing the obvious choice. This analysis plays a crucial role in quantifying the results, enabling users to understand the limitations of the two annealing methods for different materials. By identifying the best practices, users can achieve optimal results tailored to specific applications, thereby improving the efficiency and performance of the manufacturing process.

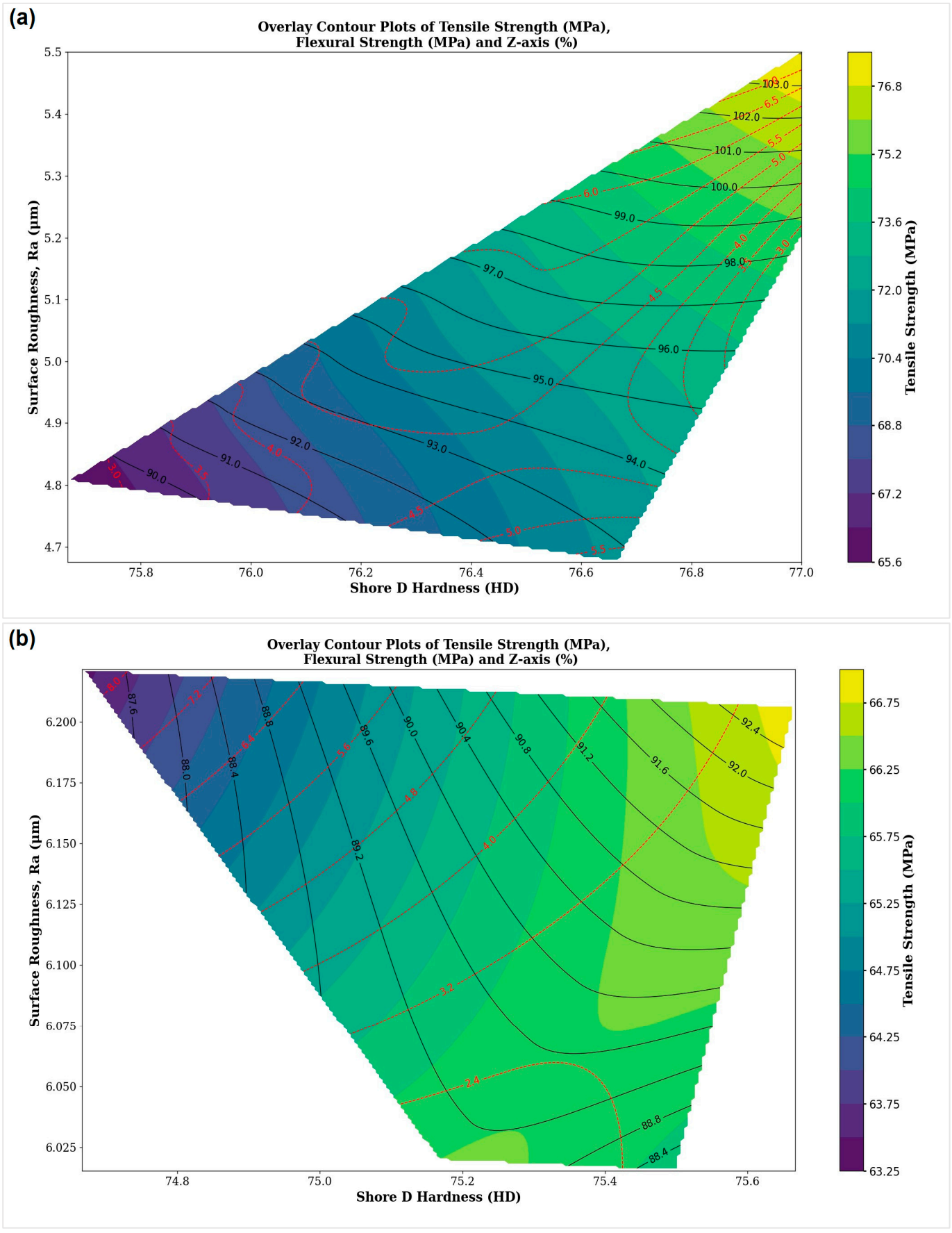

Figure 6. Overlay contour plots for PAHT-CF: (**a**) oven annealing; (**b**) sand annealing.

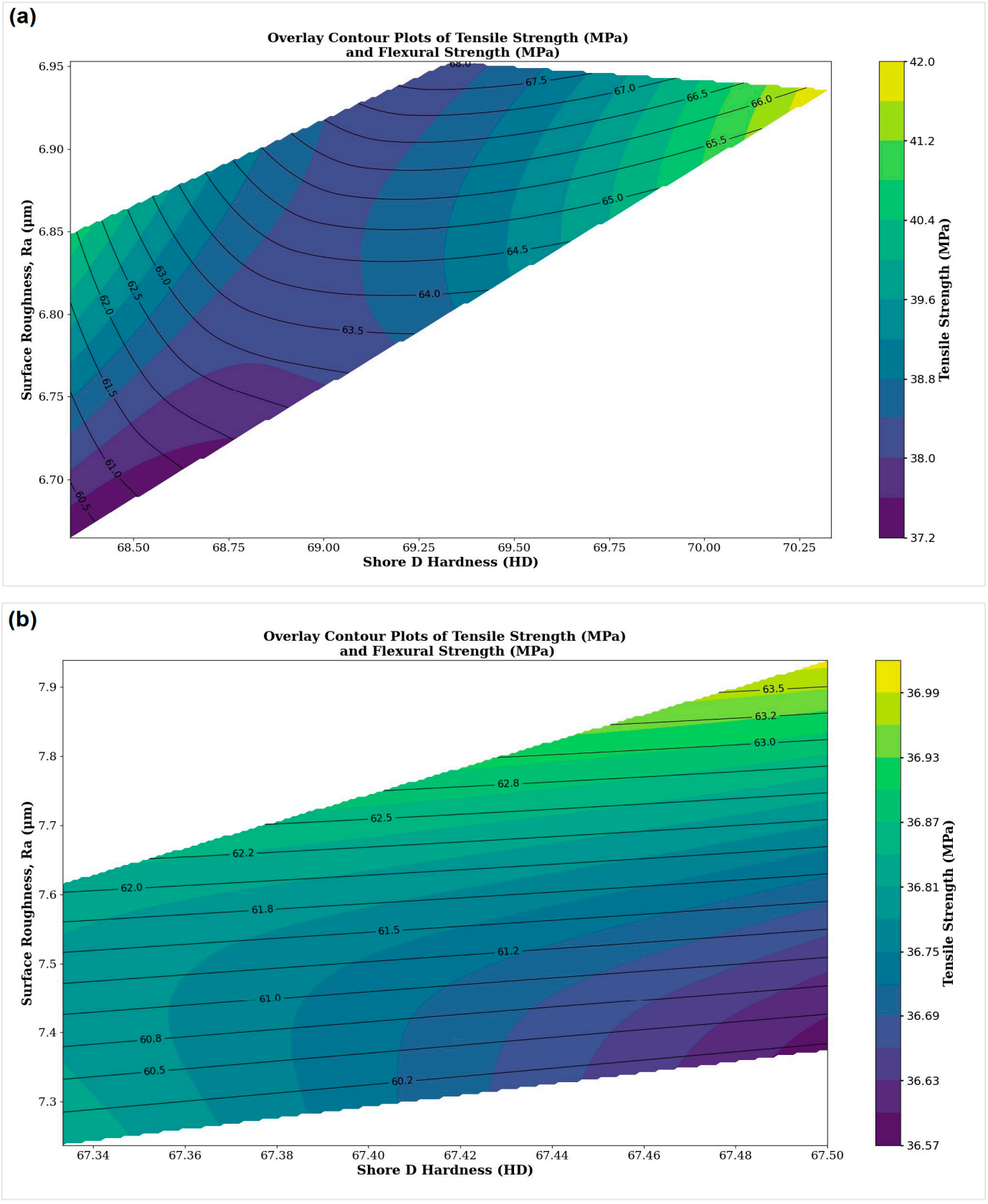

Figure 7. Overlay contour plots for PETG-CF: (**a**) oven annealing; (**b**) sand annealing.

5. Conclusions

This study provides a novel comparative analysis of two annealing methods, i.e., conventional oven annealing and fluidized bed annealing with sharp sand on FFF-printed carbon-fiber-reinforced polymers, including semi-crystalline (PLA-CF and PAHT-CF,) and amorphous (PETG, CF and ABS-CF) materials. By examining key properties such as dimensional stability, tensile strength, surface roughness, hardness, and flexural strength, the study not only highlights each method's advantages and limitations for specific composite types but also identifies optimal annealing parameters. This dual-method approach offers a tailored strategy for post-processing FFF composites, expanding alternatives to conventional oven annealing and improving the performance and reliability of 3D-printed composites in engineering applications. The following conclusions were drawn from the study:

1. Sand annealing provided better dimensional stability to all the composites (except PLA-CF due to its low thermal stability), whereas oven annealing showed deviations along the *z*-axis as high as 18% for ABS-CF, compared to 7.58% observed for sand annealing at the highest annealing temperature of 125 °C.
2. The controlled and uniform heating of oven annealing demonstrated better surface finish compared to sand annealing. The surface roughness values increased with increasing annealing temperatures for oven annealing, but sand annealing showed consistent albeit higher values for all the composites.
3. Tensile testing demonstrated the effectiveness of oven annealing over sand annealing with higher tensile strengths in all cases. For the semi-crystalline materials, the tensile strength increased with increasing annealing temperature. However, the amorphous materials showed a decline at the highest annealing temperature as excessive temperature can soften the material without significantly increasing strength.
4. The difference between the two annealing methods in terms of hardness values is minimal, indicating their effectiveness in enhancing this aspect for the composites at all temperatures.
5. Oven annealing showed higher flexural strength for all the four composites that increased with increasing annealing temperatures. Sand annealing also demonstrated a similar pattern albeit with lower values, compared to oven annealing.

For future work, the parameters could be changed to ascertain the impact of the different annealing methods. These changes include increasing the annealing time interval and temperature as well as changing the type of sand used and the depth at which the samples are submerged. By carefully manipulating these variables, the performance of the printed carbon-fiber-based composites can be significantly enhanced. This level of control allows manufacturers to refine printed parts to meet the specific demands of high-performance functional applications. As a result, the tailored composites can meet stringent requirements, including increased load-bearing capacity and dimensional stability, making them ideal for use in challenging environments where standard materials would fail.

Author Contributions: J.B. conceptualized the idea, designed the methodology, and undertook data curation, investigation, resource acquisition, formal analysis, project administration, and manuscript writing, reviewing, and editing; M.A.A.K., M.A., and V.M. undertook data curation, investigation, and formal analysis. All authors have read and agreed to the published version of the manuscript.

Funding: This research did not receive any external funding.

Data Availability Statement: The data can be made available on reasonable request.

Conflicts of Interest: Author V.M. was employed by MG Electric (Colchester) Ltd. company. The remaining authors declare that the research was conducted without any commercial or financial relationships that could be construed as potential conflicts of interest.

References

1. Kanishka, K.; Acherjee, B. Revolutionizing manufacturing: A comprehensive overview of additive manufacturing processes, materials, developments, and challenges. *J. Manuf. Process.* **2023**, *107*, 574–619. [CrossRef]
2. Butt, J.; Mohaghegh, V. Combining digital twin and machine learning for the fused filament fabrication process. *Metals* **2022**, *13*, 24. [CrossRef]
3. Butt, J.; Onimowo, D.A.; Gohrabian, M.; Sharma, T.; Shirvani, H. A desktop 3D printer with dual extruders to produce customised electronic circuitry. *Front. Mech. Eng.* **2018**, *13*, 528–534. [CrossRef]
4. Bahnini, I.; Rivette, M.; Rechia, A.; Siadat, A.; Elmesbahi, A. Additive manufacturing technology: The status, applications, and prospects. *Int. J. Adv. Manuf. Technol.* **2018**, *97*, 147–161. [CrossRef]
5. First Metal Part 3D Printed in Space. Available online: https://phys.org/news/2024-09-metal-3d-space.html#:~:text=Additive%20manufacturing%20in%20space%20will,relying%20on%20resupplies%20and%20redundancies (accessed on 24 September 2024).
6. How Barrelhand Is Using Additive Manufacturing to Redefine Space Tools—Interview with Karel Bachand. Available online: https://www.3printr.com/how-barrelhand-is-using-additive-manufacturing-to-redefine-space-tools-interview-with-karel-bachand-3274073/ (accessed on 24 September 2024).
7. *ISO/ASTM 52900:2021*; Additive Manufacturing—General Principles—Fundamentals and Vocabulary; International Organization for Standardization: Geneva, Switzerland, 2021.
8. Oleff, A.; Küster, B.; Stonis, M.; Overmeyer, L. Process monitoring for material extrusion additive manufacturing: A state-of-the-art review. *Prog. Addit. Manuf.* **2021**, *6*, 705–730. [CrossRef]
9. Butt, J.; Bhaskar, R.; Mohaghegh, V. Investigating the influence of material extrusion rates and line widths on FFF-printed graphene-enhanced PLA. *J. Manuf. Mater. Process.* **2022**, *6*, 57. [CrossRef]
10. Kallel, A.; Koutiri, I.; Babaeitorkamani, E.; Khavandi, A.; Tamizifar, M.; Shirinbayan, M.; Tcharkhtchi, A. Study of bonding formation between the filaments of PLA in FFF process. *Int. Polym. Process.* **2019**, *34*, 434–444. [CrossRef]
11. Butt, J.; Bhaskar, R.; Mohaghegh, V. Investigating the effects of extrusion temperatures and material extrusion rates on FFF-printed thermoplastics. *Int. J. Adv. Manuf. Technol.* **2021**, *117*, 2679–2699. [CrossRef]
12. Butt, J.; Bhaskar, R.; Mohaghegh, V. Analysing the effects of layer heights and line widths on FFF-printed thermoplastics. *Int. J. Adv. Manuf. Technol.* **2022**, *121*, 7383–7411. [CrossRef]
13. Shakeri, Z.; Benfriha, K.; Shirinbayan, M.; Ahmadifar, M.; Tcharkhtchi, A. Mathematical modeling and optimization of fused filament fabrication (FFF) process parameters for shape deviation control of polyamide 6 using Taguchi method. *Polymers* **2021**, *13*, 3697. [CrossRef]
14. Vidakis, N.; Kechagias, J.D.; Petousis, M.; Vakouftsi, F.; Mountakis, N. The effects of FFF 3D printing parameters on energy consumption. *Mater. Manuf. Process.* **2023**, *38*, 915–932. [CrossRef]
15. Heidari-Rarani, M.; Rafiee-Afarani, M.; Zahedi, A.M. Mechanical characterization of FDM 3D printing of continuous carbon fiber reinforced PLA composites. *Compos. Part B Eng.* **2019**, *175*, 107147. [CrossRef]
16. Yu, S.; Hwang, Y.H.; Hwang, J.Y.; Hong, S.H. Analytical study on the 3D-printed structure and mechanical properties of basalt fiber-reinforced PLA composites using X-ray microscopy. *Compos. Sci. Technol.* **2019**, *175*, 18–27. [CrossRef]
17. Abderrafai, Y.; Mahdavi, M.H.; Sosa-Rey, F.; Hérard, C.; Navas, I.O.; Piccirelli, N.; Lévesque, M.; Therriault, D. Additive manufacturing of short carbon fiber-reinforced polyamide composites by fused filament fabrication: Formulation, manufacturing and characterization. *Mater. Des.* **2022**, *214*, 110358. [CrossRef]
18. Chicos, L.A.; Pop, M.A.; Zaharia, S.M.; Lancea, C.; Buican, G.R.; Pascariu, I.S.; Stamate, V.M. Infill density influence on mechanical and thermal properties of short carbon fiber-reinforced polyamide composites manufactured by FFF process. *Materials* **2022**, *15*, 3706. [CrossRef] [PubMed]
19. Arjun, P.; Bidhun, V.K.; Lenin, U.K.; Amritha, V.P.; Pazhamannil, R.V.; Govindan, P. Effects of process parameters and annealing on the tensile strength of 3D printed carbon fiber reinforced polylactic acid. *Mater. Today Proc.* **2022**, *62*, 7379–7384. [CrossRef]
20. Bhandari, S.; Lopez-Anido, R.A.; Gardner, D.J. Enhancing the interlayer tensile strength of 3D printed short carbon fiber reinforced PETG and PLA composites via annealing. *Addit. Manuf.* **2019**, *30*, 100922. [CrossRef]
21. Seok, W.; Jeon, E.; Kim, Y. Effects of annealing for strength enhancement of FDM 3D-printed ABS reinforced with recycled carbon fiber. *Polymers* **2023**, *15*, 3110. [CrossRef]
22. Bambu Filament: PLA-CF. Available online: https://cdn.shopify.com/s/files/1/0584/7236/6216/files/Bambu_PLA-CF_Technical_Data_Sheet_V3.pdf (accessed on 25 September 2024).
23. Bambu Filament: PAHT-CF. Available online: https://cdn.shopify.com/s/files/1/0584/7236/6216/files/Bambu_PAHT-CF_Technical_Data_Sheet_V2.pdf (accessed on 25 September 2024).
24. Bambu Filament: PETG-CF. Available online: https://cdn.shopify.com/s/files/1/0584/7236/6216/files/Bambu_PETG-CF_Technical_Data_Sheet_V2.pdf (accessed on 25 September 2024).
25. IEMAI: ABS-CF Technical Data Sheet. Available online: https://store.iemai3d.com/wp-content/uploads/2024/01/06_CF-ABS-Filament-TDS-1.pdf (accessed on 25 September 2024).
26. *BS EN ISO 527-2:2012*; Plastics—Determination of Tensile Properties–Part 2: Test Conditions for Moulding and Extrusion Plastics; British, European and International Standard: London, UK, 2012.
27. *BS EN ISO 868:2003*; Plastics and Ebonite–Determination of Indentation Hardness by Means of a Durometer (Shore Hardness). British, European and International Standard: London, UK, 2018.

28. *BS EN ISO 178:2019*; Plastics—Determination of Flexural Properties. British, European and International Standard: London, UK, 2019.
29. Butt, J.; Bhaskar, R. Investigating the effects of annealing on the mechanical properties of FFF-printed thermoplastics. *J. Manuf. Mater. Process.* **2020**, *4*, 38. [CrossRef]
30. Mitutoyo: SJ-210—Portable Surface Roughness Tester. Available online: https://www.mitutoyo.com/products/form-measurement-machine/surface-roughness/sj-210-portable-surface-roughness-tester-2/ (accessed on 16 September 2024).
31. *ISO 21920-2:2021*; Geometrical Product Specifications (GPS)—Surface Texture: Profile—Part 2: Terms, Definitions and Surface Texture Parameters. International Organization for Standardization (ISO): Geneva, Switzerland, 2021.
32. Hart, K.R.; Dunn, R.M.; Sietins, J.M.; Mock, C.M.H.; Mackay, M.E.; Wetzel, E.D. Increased fracture toughness of additively manufactured amorphous thermoplastics via thermal annealing. *Polymer* **2018**, *144*, 192–204. [CrossRef]
33. Cao, M.; Cui, T.; Yue, Y.; Li, C.; Guo, X.; Jia, X.; Wang, B. Preparation and characterization for the thermal stability and mechanical property of PLA and PLA/CF samples built by FFF approach. *Materials* **2023**, *16*, 5023. [CrossRef] [PubMed]
34. Ivey, M.; Melenka, G.W.; Carey, J.P.; Ayranci, C. Characterizing short-fiber-reinforced composites produced using additive manufacturing. *Adv. Manuf. Polym. Compos. Sci.* **2017**, *3*, 81–91. [CrossRef]
35. Alsoufi, M.S.; Elsayed, A.E. How surface roughness performance of printed parts manufactured by desktop FDM 3D printer with PLA+ is influenced by measuring direction. *Am. J. Mech. Eng* **2017**, *5*, 211–222.
36. Garg, A.; Bhattacharya, A.; Batish, A. On surface finish and dimensional accuracy of FDM parts after cold vapor treatment. *Mater. Manuf. Process.* **2016**, *31*, 522–529. [CrossRef]
37. Tate, J.S.; Brushaber, R.P.; Danielsen, E.; Kallagunta, H.; Navale, S.V.; Arigbabowo, O.; Shree, S.; Yaseer, A. *Electrical and Mechanical Properties of Fused Filament Fabrication of Polyamide 6/Nanographene Filaments at Different Annealing Temperatures*; University of Texas at Austin: Austin, TX, USA, 2019.
38. Valvez, S.; Reis, P.N.; Ferreira, J.A. Effect of annealing treatment on mechanical properties of 3D-Printed composites. *J. Mater. Res. Technol.* **2023**, *23*, 2101–2115. [CrossRef]
39. Nassar, A.; Younis, M.; Elzareef, M.; Nassar, E. Effects of heat-treatment on tensile behavior and dimension stability of 3d printed carbon fiber reinforced composites. *Polymers* **2021**, *13*, 4305. [CrossRef]